LAWRENCE
LIVERMORE
NATIONAL
LABORATORY

LLNL-JRNL-412819

Interfacial behavior of perchlorate versus chloride ions in saturated aqueous salt solutions

S. Ghosal, I.-F. W. Kuo, M. D. Baer, H. Bluhm

May 6, 2009

The Journal of Physical Chemistry B

Disclaimer

Interfacial behavior of perchlorate versus chloride ions in saturated aqueous salt solutions

Sutapa Ghosal[1*], I-Feng William Kuo[1], Marcel D. Baer[2], Hendrik Bluhm[3]

[1]Physical and Life Sciences Directorate, Lawrence Livermore National Laboratory, L-437, Livermore CA 94551, USA

[2]Lehrstuhl fur Theoretische Chemie, Ruhr-Universitat Bochum, 44780 Bochum, Germany

[3]Chemical Sciences Division, Lawrence Berkeley National Laboratory, Berkeley, CA 94720

* corresponding author: ghosal2@llnl.gov

Abstract

In recent years combination of theoretical and experimental work have presented a novel view of the aqueous interface wherein hard and/or multiply charged ions are excluded from the interface, but large polarizable anions show interfacial enhancement relative to the bulk. The observed trend in the propensity of anions to adsorb at the air/water interface appears to be reverse of the Hofmeister series for anions. This study focuses on experimental and theoretical examination of the partitioning behavior of perchlorate (ClO_4^-) and chloride (Cl^-) ions at the air/water interface. We have used ambient pressure X-ray photoelectron spectroscopy technique to directly probe the interfacial concentrations of ClO_4^- and Cl^- ions in sodium perchlorate and sodium chloride solutions, respectively. Experimental observations are compared with first principles molecular dynamics simulations. Both experimental and simulation results show enhancement of ClO_4^- ion at the interface, compared with the absence of such enhancement in the case of Cl^- ion. These observations are in agreement with the expected trend in the interfacial propensity of anions based on the Hofmeister series.

Introduction

There is a steadily growing body of research suggesting that the propensity of anions to adsorb to the air/water interface follows an inverse order of the Hofmeister series for anions: $SO_4^{2-} > F^- > HPO_4^{2-} > CH_3COO^- > Cl^- > Br^- > NO_3^- > ClO_3^- > I^- > ClO_4^- > SCN^-$.(1) Recent theoretical and experimental work all point towards an emerging picture wherein hard and/or multiply charged ions are excluded from the air/water interface, while large polarizable anions show enhanced presence at the interface relative to the bulk. (2-11) The propensity of large, polarizable ions for aqueous interfaces is contrary to the traditional view of an ion-free interface (12, 13) and as such has garnered considerable research interest. Also, the presence of ions at aqueous interfaces has important consequences for heterogeneous physics and chemistry relevant to both technology and environmental processes. For instance, atmospheric chemistry of aqueous sea salt is now known to be driven by the presence of halide ions at the air/water interface.(8, 14)

The present study examines the propensity of perchlorate (ClO_4^-) and chloride (Cl^-) ions for the air/water interface. ClO_4^- is expected to show enhanced presence at the solution interface on the basis of its relative position in the Hofmeister series. Historically, the presence of ClO_4^- ions near the air/water interface had been proposed as early as 1957 based on the negative surface potential measurements of aqueous solution of alkali metal perchlorate salt. (15) Recent studies have also proposed the interfacial enhancement of ClO_4^- based on mass spectrometry, vibrational sum frequency spectroscopy and surface potential measurements.(16, 17) However, to the best of our knowledge there has been no direct experimental observation of the propensity of ClO_4^-

ions for the air/water interface yet. In contrast to ClO_4^-, molecular dynamics (MD) simulations of alkali halide solutions propose that the Cl^- ion is neutral with respect to its propensity for the interface, *i.e.* it is neither enhanced nor depleted at the interface relative to the bulk solution.(18)

In addition to its proposed interfacial behavior in aqueous solution, ClO_4^- is also a known natural and anthropogenic contaminant with the potential to cause hypothyroidism in humans. In recent years it has attracted considerable attention as an emerging environmental pollutant responsible for the widespread contamination of groundwater, particularly in the southwestern United States.(19-21) Physical and chemical characteristics of ClO_4^- such as its extreme solubility and non-reactivity (due to large activation energies) make it a difficult ion to uniquely analyze for and remediate.(19) As a result there is considerable interest in devising new technologies for the effective treatment of ClO_4^- contamination of water. In this context, detailed knowledge of the behavior of ClO_4^- ion in aqueous solution constitutes an essential step towards the development of a potentially viable remediation technology such as the selective extraction of contaminants naturally enriched at the air/water interface.

In recent years applications of various surface sensitive experimental techniques have yielded a wealth of information regarding the nature and interaction of ions at aqueous interfaces. (2, 6, 9) We have previously reported *in-situ* observation of the interfacial enhancement of larger, more polarizable halide ions, *i.e.* Br^- and I^- in aqueous salt solutions based on ambient pressure X-ray photoelectron spectroscopy (AP-XPS) technique. (2, 22) AP-XPS combines the surface-sensitivity of conventional XPS analysis with the ability to acquire photoemission spectra in gaseous environments at pressures up

to several Torrs. (23) This makes it a particularly suitable technique for probing ion distribution in the surface region of aqueous solutions. In this study we have used AP-XPS to directly probe the relative and absolute concentrations of ClO_4^- and Cl^- ions at the air/water interface of aqueous sodium perchlorate ($NaClO_4$) and sodium chloride (NaCl) solutions, respectively. Our results show enhancement of the ClO_4^- ion at the air/solution interface and the absence of such an enhancement in the case of Cl^- ion. Additionally, experimental observations for the ClO_4^- ion are compared with first principles molecular dynamics (MD) simulations. Simulation results confirm the experimentally observed interfacial enhancement of the ClO_4^- ion in solution. Therefore, our observations are in agreement with the expected trend in terms of the interfacial propensity of anions based on the Hofmeister series.

Experimental Details

Ambient Pressure XPS

The AP-XPS system has been described in detail elsewhere (23, 24) and only a brief description of the features pertinent to our experiments is given here. The AP-XPS system is equipped with a differentially pumped electrostatic transfer lens system which enables the acquisition of photoemission spectra at pressures up to several Torr. This feature is critical for making in situ measurements on aqueous solutions in equilibrium with water vapor. An aqueous salt solution was generated *in situ*, starting with dry crystalline salt and progressively increasing the relative humidity (RH) in the chamber until formation of the solution phase was observed and subsequently confirmed by the appearance and growth of the condensed phase peak in the O(1s) spectra. The requisite

RH conditions for $NaClO_4$ and NaCl dissolution were achieved by lowering the sample temperature while maintaining a given water vapor pressure in the chamber. The sample temperature (read by a thermocouple attached to the bottom of the salt crystals) and water vapor pressure (read by a capacitance pressure gauge) were carefully controlled throughout the experiment to ensure continued presence of the solution phase. In the case of $NaClO_4$, water vapor pressure and sample temperature corresponding to deliquescence were ~1.7 Torr and ~-7 °C, respectively. The corresponding values for NaCl deliquescence were ~1.6 Torr and ~-10 °C.

In XPS, probe depth into the sample is determined by the inelastic mean free path (IMFP) of the ejected photoelectrons, which is a function of the photoelectron kinetic energy (PKE). PKE in turn is determined by the incident photon energy. Beamline 11.0.2. at the Advanced Light Source, where the AP-XPS measurements were made, provides tunable X-ray energies in the range from 90 to 2100 eV. In our experiments depth dependent density profiles of ions in solution were measured by varying the kinetic energy of the photoelectrons to probe different depths into the solution. The IMFP of photoelectrons in liquids is not well understood and accurate estimates remain difficult to obtain (25) However, based on the properties of neat water we estimated that for the lowest PKE (200 eV) IMFP is equivalent to the outermost 5-11 Å, whereas at the highest PKE (600 eV) it is equal to the outermost 20-30 Å of solution.(26) For the direct comparison of elemental compositions corresponding to a single probe depth, spectra of all the elements were acquired with the same PKE value at the same sample location consecutively. This methodology has been used previously to demonstrate preferential enhancement of the larger halide ions (Br^-, I^-) at the air/solution interface. (2, 22)

First Principles Molecular Dynamics Simulations

Potential of mean force (PMF) calculation for the transport of ClO_4^- ion across the liquid-vapor interface was carried out by constraining the ClO_4^- ion to different interfacial depths within a simulated water slab to model ion transport across the liquid-vapor interface. The water slab consisted of 216 water molecules residing within a simulation cell of 15 Å X 15 Å X 71.44 Å. More details regarding the simulation protocols for aqueous interfacial calculations can be found elsewhere.(27, 28) The PMF calculation was constructed of 26 independent first principles molecular dynamics simulations (FPMD) wherein the ion was constrained at a series of 1.06 Å intervals as a function of interfacial depth. Each independent FPMD simulation was run for a total of 5-10 ps wherein the relative position of the ClO_4^- ion as a function of interfacial depth was maintained. In addition, a ClO_4^- ion solvated by 64 water molecules was also simulated with 3-D periodic boundary condition in the isobaric-isothermal ensemble (NpT) to mimic bulk solvation environment. The condensed phase simulation was run for a total of 11 ps.

FPMD simulations were performed using Kohn-Sham formulation of density functional theory as implemented in the QuickStep module of CP2K.(29, 30) The FPMD simulations use a dual basis set method where the valence states are described using both Gaussian type orbitals (TZV2P) as well as plane-wave basis set expanded up to 280 Ry cutoff for the density.(31) The core electronic states are represented by Goedecker-Teeter-Hutter type pseudopotentials.(32) This combination has been shown to be both computationally cost effective and accurate in reproducing different results from plane-wave basis calculations for aqueous solutions.(33) Efficient iterative solver as well as

wavefunction extrapolation was utilized to reduce the average number of iterations required during the SCF cycle for each molecular dynamics step.(34)

Molecular Dynamics Simulations

In addition FPMD, molecular dynamics simulation utilizing polarizable force fields was performed on a 1 M $NaClO_4$ solution following the approach of Jungwirth and Tobias.(35) The three-site water model of Caldwell and Kollman which includes polarization effects was utilized.(36) The atomic polarizability α (α_{Cl} =0.2, α_O=0.4) and charge q (q_{Cl} = 1.2 *e*, q_O =-0.55 *e*) for ClO_4^- was determined from gas phase calculations utilizing Gaussian98.(37) Intramolecular parameters (r_{ClO}= 1.495 Å, k_{bond} = 360 kcal/mol; θ_{OClO} = 109.5°, k_{bend} = 140 kcal/mol) were fitted to match the power spectra obtained from the condensed phase FPMD simulation of ClO_4^- in the isothermal-isobaric ensemble. Explicit nonbonded oxygen(ClO_4^-)-oxygen(water) LJ interaction parameters (ϵ = 1.9 Å; σ = 0.154) were obtained by fitting to the radial distribution function of the condensed phase FPMD simulation, while the chlorine-oxygen(water) LJ interaction parameters were set to zero. The newly parameterized polarizable model for ClO_4^- ion was able to accurately reproduce the condensed phase structure of ClO_4^- ion in the bulk when compared to the condensed phase FPMD simulation. To build up an interface the system containing 16 Na^+ and 16 ClO_4^- were solvated with 1054 water molecules (~1M) and equilibrated within the isothermal-isobaric ensemble at 400 K and 1 atm using periodic boundary conditions. After 1 ns the box was extended in the *z* direction (25 Å x 25 Å x 80 Å) and the water lamella placed in the center. The interface was simulated for 6 ns using a time-step of 1 fs.

Results and Discussion

Sodium Perchlorate ($NaClO_4$)

Photoinduced decomposition of $NaClO_4$: Fig 1 shows a series of photoemission spectra of the Cl(2p) region acquired sequentially at the same location on a dry $NaClO_4$ crystallite. The incident photon energy of 500 eV corresponds to a PKE of 300 eV. From measurements of the photon flux using a calibrated photo diode we estimate the flux density to be 5×10^{12} photons$\bullet s^{-1}\bullet cm^{-2}$. The spectra shown in Fig. 1 have been charge referenced to the Na (2s) binding energy (BE) of 64.20 eV. (38) Increasing exposure to incident x-rays alters the chemistry of the Cl containing species. This is evident from the appearance of additional spectral features corresponding to chlorate (ClO_3^-) and chloride (Cl^-) species, along with ClO_4^-. Peak intensities associated with the various species (ClO_4^-, ClO_3^-, Cl^-) are dependent on the x-ray exposure time, *i.e.* ClO_4^- peak intensity decreases with increasing exposure while the ClO_3^- and Cl^- peaks grow in intensity over time. However, spectra acquired at previously unexamined (new) locations on the sample are dominated by the ClO_4^- peak and show minimal presence of ClO_3^- and Cl^- species. The observed behavior is the result of photoinduced decomposition of ClO_4^- ion into ClO_3^- and Cl^- species and has been reported previously by Copperwaite *et al.* (39) Based on their observations Copperwaite *et al.* concluded that the "photoinduced decomposition of ClO_4^- proceeds via simple consecutive first-order processes involving ClO_3^- as an intermediate." In the case of NaCl, we have also previously observed similar photoinduced loss of Cl^- species as a function of x-ray exposure.

Fig 2 shows a plot of the normalized relative concentrations of ClO_4^-, ClO_3^-, and Cl^- species as a function of the x-ray exposure time. Sensitivity factor for the

normalization procedure was determined experimentally based on the integrated XP spectral areas corresponding to ClO_4^-, ClO_3^-, and Cl^- species and setting the sum of these individual spectral areas equal to 1 for each measurement. The experimentally derived sensitivity factor was then used to normalize individual spectral areas corresponding to the different species. Fitting of the normalized relative concentration of ClO_4^- as a function of x-ray exposure time gives first order rate and time constants of 0.6 min^{-1} and 1.6 min respectively, for the photoinduced decomposition process. The value of rate constant measured in our experiment is significantly greater than that reported by Copperwaite *et al* (2.06 x 10^{-3} min^{-1}). (26) The relatively larger rate constant for the photoinduced decomposition of ClO_4^- measured in our experiment is most likely the result of considerably larger photon flux density associated with synchrotron radiation compared to a laboratory based x-ray source such as the one used by Copperwaite *et al.* (40)

Due to the potential for photoinduced decomposition of ClO_4^- and Cl^- species in our experiments, several precautionary measures were taken to minimize such loss. Each set of spectra (Cl2p, Na2s, O1s) for a given PKE was taken at a fresh spot on the sample, where the Cl(2p) spectrum was always acquired first, and the acquisition time was limited to less than a minute. Also, it is worth noting that increased ionic mobility associated with the solution phase helps to heal the photoinduced loss and thereby reduces its effect on the experimental results.

Depth resolved distribution of ClO_4^- ion in an aqueous $NaClO_4$, solution. To determine the propensity of ClO_4^- ions for the solution/vapor interface, we used AP-XPS

to measure depth resolved distribution of ions in aqueous $NaClO_4$ solution. Relative concentrations of the various ions as a function of depth into the solution were determined based on XP spectra corresponding to Na(2s), Cl(2p) and O(1s) regions, acquired at PKEs of 200, 300, 400, and 600 eV. Fig. 3 presents XP spectra corresponding to the O(1s), Cl(2p) and Na(2s) core levels for a saturated $NaClO_4$ solution at 200 eV PKE. The use of a range of PKE values enabled us to probe different depths into the solution, the lowest energy being the most surface sensitive (5-11 Å) and the highest PKE being most representative of the bulk (20-30 Å).(4, 18) In these experiments, quantitative depth dependent distributions of ClO_4^- ions in the solution are expressed as ClO_4^-/Na^+ and ClO_4^-/O ratios. The ratios were determined from the corresponding integrated XP spectral areas, and normalized using the approach outlined below. For dry $NaClO_4$ crystallite, the ClO_4^-(Cl2p)/Na^+(Na2s) and ClO_4^-(Cl2p)/O(O1s) ratios are expected to be 1 and 0.25, respectively, independent of the probe depth. Based on this, sensitivity factors for the normalization of ClO_4^-/Na^+ and ClO_4^-/O ratios measured in our experiment were determined from the Cl(2p), Na(2s) and O(1s) XP spectra acquired on dry (~10% relative humidity) $NaClO_4$ crystallites. The experimentally determined sensitivity factors were subsequently used to normalize ClO_4^-/Na^+ and ClO_4^-/O peak area ratios measured for the aqueous $NaClO_4$ solution. The normalized ClO_4^-/O ratio as a function of PKE (obtained using the O(1s) peak area associated with condensed phase liquid water) is representative of the absolute concentration of ClO_4^- as a function of depth into the solution. However, the authors would like to point out that the O(1s) peak associated with condensed phase water (535 eV BE) overlaps with the O(1s) peak from the ClO_4^- ion (533 eV BE). As a result, the O(1s) peak area for the condensed phase water includes minimal, but finite

contribution from the ClO_4^- related O(1s) species, thereby resulting in a slight overestimation of condensed phase water peak area. Therefore, it is likely that the actual ClO_4^- concentration in the solution is slightly greater than our calculated value. However, this is true for all experimental probe depths and as such does not interfere with the depth dependent comparison of the ClO_4^- concentration in the solution. The experimentally measured depth dependent distribution of ClO_4^- ions in solution are shown in Fig. 4 where we have plotted the ClO_4^-/Na^+ ratio as well as the absolute ClO_4^- concentration as a function of the PKE. Both, the ClO_4^-/Na^+ ratio and the absolute concentration of ClO_4^- in the solution decrease with increasing PKE, with the highest value corresponding to the lowest PKE. The observed trend is indicative of the interfacial enhancement ClO_4^- ion relative to the bulk solution and to the cation (Na^+).

While precautions were taken to minimize photoinduced decomposition of ClO_4^- during measurement, the Cl(2p) spectral region showed small but finite contributions from the decomposition products namely, ClO_3^-, and Cl^-. The effect of photo-induced decomposition was accounted for in the quantification process by using only the Cl(2p) peak area associated with the ClO_4^- species to calculate relative and absolute concentrations of ClO_4^- in the solution. Preferential photo-induced loss of ClO_4^- ions relative to Na and O is likely to have resulted in an underestimation of the ClO_4^- ion concentration in these measurements. Therefore, in the absence of photoinduced decomposition one would expect the observed interfacial enrichment of ClO_4^- ions to be greater than that shown in Fig 4.

Comparison of the ClO_4^- and Na^+ ion concentrations (expressed as ClO_4^-/O and Na^+/O ratios, respectively) measured in our experiment with the values expected based

on bulk thermodynamic data for a saturated $NaClO_4$ solution in the absence of ClO_4^- interfacial enhancement is shown in Fig. 5. The concentration values expected for a bulk saturated solution (3.5 M) were determined based on salt solubility data at the appropriate temperature (-6.8 °C).(11) The interfacial concentration (at PKE 200 eV) of ClO_4^- ions measured in our experiment is significantly greater than the value expected for a saturated $NaClO_4$ solution, while the measured bulk ClO_4^- concentration (at PKE 600 eV) is in agreement with the saturated solution. Hence, our results show that in aqueous $NaClO_4$ solution ClO_4^- ions have enhanced presence at the solution/vapor interface relative to the concentration expected for a saturated solution based on thermodynamic data.

Comparison of experiment with simulation results.

The enhancement of ClO_4^- ion at the liquid-vapor interface is also supported by results from the FPMD simulations. Preferential solvation sites for ClO_4^- ion in the water slab can be gleaned from Fig. 6 where the average force, $\langle F_z \rangle$, exerted on ClO_4^- as a function of depth is shown. A value close to zero indicates that there is minimal force acting on the ion in the *z* direction and thus represents a stable solvation site or local minimum. Based on the values of $\langle F_z \rangle$ shown in Fig. 6 the ClO_4^- ion has two stable solvation sites located, 1) at the center of the slab (~-15 Å) and, 2) at the interfacial region (~3 Å) (the Gibbs dividing surface (GDS) is set to 0.0 Å). However, based on the computed $\langle F_z \rangle$ from FPMD simulations, the ClO_4^- ion is more stable at the interface relative to the bulk by ~ 16 kcal/mol. The FPMD simulations were mono ionic consisting

of a single ClO_4^- ion in the water slab and therefore screening or high ionic concentration effects were ignored.

In addition to the FPMD simulations, polarizable force field based MD simulations also show a large surface enhancement for ClO_4^- ion at the liquid-vapor interface. The density profiles computed from the MD simulation are shown in Fig. 7, which shows an enhancement of ClO_4^- ion at the liquid-vapor interface. Specifically, the polarizable force field based MD simulations predicts a maximum density of ~2.2 g/ml at approximately -0.5 Å and with an overall relative enhancement of ~9 when compared to bulk density of ClO_4^- (~0.25 g/ml). Although both FPMD and polarizable force field based MD simulations predict surface enhancement of ClO_4^-, it is interesting to note that FPMD predicts that ClO_4^- ion is situated above the GDS (z = 3 Å) whereas polarizable force field predicts maximum enhancement slightly below the GDS (z = -0.5 Å). This disparity could be due to the limitation of the polarizable force field to describe partial solvation as would occur above the GDS. Overall, both simulation methods are in good agreement with the AP-XPS based experiments wherein surface enhancement of ClO_4^- ions in solution was measured directly.

Fig. 8 shows a quantitative comparison between the AP-XPS experiment and the polarizable force field based MD simulation results. For the purpose of comparison the theoretical ion densities as predicted by MD simulation were converted into simulated XPS ionic ratios using the convolution integral,

$$\int e^{\left(\frac{-z}{\Gamma(PKE)}\right)}\rho(z)dz$$

where z is the distance into the solution from the solution/vapor interface, ρ(z) is the ion density as a function of depth into solution, obtained from the results of the MD simulations, and Γ(PKE) is the IMFP of the photoelectrons which is a function of the PKE.(25) Both AP-XPS experiment and simulation results show decrease in the ClO_4^- /Na^+ ratio with increasing PKE thereby indicating preferential enhancement of ClO_4^- at the solution interface relative to the bulk. While both theory and experiment show similar trend in ClO_4^-/Na^+ ratio as a function of PKE, the actual numbers differ in magnitude. The observed discrepancy between experimentally measured and theoretically predicted ion ratios (Fig. 6) may be a result of the difference in solution concentrations probed in the experiment versus the simulation – saturated versus unsaturated solution, respectively. Also, the dependence of IMFP on PKE may be stronger than our present estimate, which in turn would influence the predicted ratios.

Depth resolved distribution of Cl^- ion in an aqueous NaCl solution. In the past decade MD simulations of aqueous interfaces have proposed that Cl^- ions in solution are neither strongly repelled nor enhanced at the solution/vapor interface.(18) We have used AP-XPS measurements to verify the proposed distribution profile of Cl^- ions in aqueous NaCl solution. Quantitative comparison of elemental distributions in the solution was accomplished using a normalization procedure similar to the one described above, i.e. by determining the experimental sensitivity factors for Cl2p/Na2s for each PKE from measurements at 5% RH, where the expected ratio for Cl/Na is 1 for all PKEs. These sensitivity factors where then used to normalize the Cl/Na ratios for the deliquesced sample, the results are shown in Fig. 9. In agreement with MD simulations, the Cl^-/Na^+

ratios measured as a function of increasing PKE, hence increasing depth into the solution, do not show any evidence of Cl^- ion enhancement at the interface. The ratios are clustered around a value of 1, independent of the probe depth. This is good agreement with the expected ratio based on MD simulations for 6.1 M NaCl solutions.

Fig. 9 shows a slight depression in the Cl^-/Na^+ ratio corresponding to PKE of 400 eV. A similar effect was also observed in the case of $NaClO_4$ solution (Fig. 4). MD simulations predict the formation of a double layer with respect to anion versus cation distributions near the solution/vapor interface. "Na^+ ions are expected to remain well solvated in the interior of the solution while Cl^- ions occupy a significant fraction of the interface."(22) Therefore, it is likely that the depression in the Cl^-/Na^+ ratio just below the interface is indicative of the proposed double layer formation. However, we would like to stress that from our data we cannot make a conclusive statement about the formation of the double layer since the small depression in the Cl^-/Na^+ (Fig. 9) and ClO_4^-/Na^+ (Fig. 4) ratios is within the margins of our experimental error. The measured depth dependent distribution of the Cl^- ions in NaCl solution appear to be in qualitative agreement with the predictions of MD simulation. Similar absence of the interfacial enhancement of Cl^- ion has been observed previously in a study involving aqueous solution of bromine doped NaCl .

Conclusion

We have used ambient pressure X-ray photoelectron spectroscopy (XPS) to examine the ion density profiles of ClO_4^- and Cl^- ions in aqueous solutions of their respective sodium salts. Our results show that ClO_4^- ions are enriched at the solution

/vapor interface relative to the bulk. The AP-XPS experimental observations are supported by FPMD and MD simulations of the solution/vapor interface of aqueous $NaClO_4$ solution. The interfacial behavior of ClO_4^- ion in solution is in contrast to that of Cl^- ions which are shown to be neutral with respect to interfacial enhancement. These observations support a growing body of research suggesting that propensity of various anions towards the solution/vapor interface follows an inverse order of the Hofmeister series. Partitioning behavior of Cl^- ions in solution has previously been examined by MD simulations as well as experimental measurements. [3, 4, 6, 10] The depth dependent distribution of Cl^- ion reported here is in agreement with these previous studies. For both Cl^- and ClO_4^- ions, the effect of photoinduced decomposition is an important consideration in using x-ray based analytical techniques such as AP-XPS. In the case of ClO_4^- we have characterized the synchrotron radiation induced loss of ClO_4^- as a function of exposure time.

This work performed under the auspices of the U.S. Department of Energy by Lawrence Livermore National Laboratory under Contract DE-AC52-07NA27344.

References

1. Hofmeister, F. (1888) On understanding of the effect of salts. Second report. On regularities in the precipitating effect of salts and their relationship to their physiological behavior *Naunyn-Schmiedebergs Arch. Exp. Pathol. Pharmakol. (Leipzig)* 24**:** 247-260.
2. Ghosal, S., Hemminger, J. C., Bluhm, H., Mun, B. S., Hebenstreit, E. L. D., Kettler, G., Ogletree, D. F., Requejo, F. G. & Salmeron, M. (2005) Electron spectroscopy of aqueous solution interfaces reveals surface enhancement of halides. *Science* 307**:** 563-66.
3. Jungwirth P, T. D. (2006) Specific ion effects at the air/water interface. *Chem. Rev.* 106**:** 1259-81.
4. Chang, T. M. & Dang, L. X. (2006) Recent advances in molecular simulations of ion solvation at liquid interfaces. *Chemical Reviews* 106**:** 1212-33.
5. Jungwirth, P. & Winter, B. (2008) Ions at aqueous interfaces: From water surface to hydrated proteins *Annual Review of Physical Chemistry* 59**:** 343-366.
6. Gopalakrishnan, S., Liu, D. F., Allen, H. C., Kuo, M. & Shultz, M. J. (2006) Vibrational spectroscopic studies of aqueous interfaces: salts, acids, bases, and nanodrops. *Chemical Reviews* 106**:** 1155–75.
7. Jungwirth, P., Finlayson-Pitts, B. J. & Tobias, D. J. (2006) Introduction: structure and chemistry at aqueous interfaces. *Chemical Reviews* 106**:** 1137–39.
8. Knipping, E. M., Lakin, M. J., Foster, K. L., Jungwirth, P., Tobias, D. J., Gerber, R. B., Dabdub, D. & Finlayson-Pitts, B. J. (2000) Experiments and simulations of ion-enhanced interfacial chemistry on aqueous NaCl aerosols *Science* 288**:** 301-306.
9. Petersen, P. B. & Saykally, R. J. (2004) Confirmation of enhanced anion concentration at the liquid water surface. *Chemical Physics Letters* 397**:** 51–55.
10. Petersen, P. B. & Saykally, R. J. (2006) On the nature of ions at the liquid water surface. *Annual Review of Physical Chemistry* 57**:** 333–64.
11. Jungwirth, P. & Tobias, D. J. (2002) Ions at the air/water interface *J. Phys. Chem. B* 106**:** 6361-6373.
12. Onasager, L. & Samaras, N. N. T. (1934) The surface tension of Debye-Huckel electrlytes. *Journal of Physical Chemistry* 2**:** 528-36.
13. Adam, N. K. (1941) *The Physics and Chemistry of Surfaces* (Oxford University Press, London).
14. Hunt, S. W., Roeselová, M., Wang, W., Wingen, L. M., Knipping, E. M., Tobias, D. J., Dabdub, D. & Finlayson-Pitts, B. J. (2004) Formation of molecular bromine from the reaction of ozone with deliquesced NaBr aerosol: Evidence for interface chemistry *Journal of Physical Chemistry A* 108**:** 11559-11572
15. Randles, J. E. B. (1957) Ionic hydration and the surface potential of aqueous electrolytes *Discuss. Faraday Soc.* 24**:** 194-99.
16. Cheng, J., Vecitis, C. D., Hoffmann, M. R. & Colussi, A. J. (2006) Experimental anion affinities for the air/water interface *J. Phys. Chem. B* 110**:** 25598-25602.
17. Gurau, M. C., Lim, S.-M., Castellana, E. T., Albertorio, F., Kataoka, S. & Cremer, P. S. (2004) On the Mechanism of the Hofmeister Effect *Journal of the American Chemical Society* 126**:** 10522-23.

18. Jungwirth, P. & Tobias, D. J. (2006) Specific ion effects at the air/water interface. *Chemical Reviews* 106**:** 1259-81.
19. Urbansky, E. T. (1998) Perchlorate Chemistry: Implications for Analysis and Remediation *Bioremediation Journal* 2**:** 81-95.
20. Urbansky, E. T. (2002) Perchlorate as an Environmental Contaminant *Environmental Science and Pollution Research* 9**:** 187-92.
21. Parker, D. R., Seyfferth, A. L. & Reese, B. K. (2008) Perchlorate in Groundwater: A Synoptic Survey of "Pristine" Sites in the Coterminous United States *Environmental Science and Technology* 42**:** 1465-71.
22. Ghosal, S., Brown, M. A., Bluhm, H., Krisch, M. J., Salmeron, M., Jungwirth, P. & Hemminger, J. C. (2008) Ion Partitioning at the liquid/vapor interface of a multi-component alkali halide solution: A model for aqueous sea salt aerosols *Journal of Physical Chemistry A* 112**:** 12378.
23. Ogletree, D. F., Bluhm, H., Lebedev, G., Fadley, C. S., Hussian, Z. & Salmeron, M. (2002) *Review of Scientific Instruments* 73**:** 3872.
24. Ogletree, D. F., Bluhm, H., Hebenstreit, E. B. & Salmeron, M. (2009) Photoelectron spectroscopy under ambient pressure and temperature conditions. *Nucl. Instrum. and Meth. A* 12**:** 155.
25. Winter, B. & Faubel, M. (2006) Photoemission from liquid aqueous solutions. *Chemical Reviews* 106**:** 1176–211.
26. Powell, C. J. & Jablonski, A. (2000) NIST Electron Inelastic-Mean-Free-Path Database,Version 1.1 *National Institute of Standards and Technology, Gaithersburg, MD, 2000*.
27. Kuo, I. F. W., Mundy, C. J., Eggimann, B. L., McGrath, M. J., Siepmann, J. I., Chen, B., Vieceli, J. & Tobias, D. J. (2006) Structure and dynamics of the aqueous liquid-vapor interface: A comprehensive particle-based simulation study *J. Phys. Chem. B* 110**:** 3738-3746.
28. Brown, M. A., D'Auria, R., Kuo, I. F. W., Krisch, M. J., Starr, D. E., Bluhm, H., Tobias, D. J. & Hemminger, J. C. (2008) Ion spatial distributions at the liquid-vapor interface of aqueous potassium fluoride solutions *Phys. Chem. Chem. Phys.* 10**:** 4778-4784.
29. CP2K.
30. VandeVondele, J., Krack, M., Mohamed, F., Parrinello, M., Chassaing, T. & Hutter, R. (2005) QUICKSTEP: Fast and accurate density functional calculations using a mixed Gaussian and plane waves approach *Comput. Phys. Commun.* 167**:** 103-128.
31. Lippert, G., Hutter, J. & Parrinello, M. (1997) A Hybrid Gaussian and Plane Wave Density Functional Scheme *Mol. Phys.* 92**:** 477.
32. Goedecker, S., Teter, M. & Hutter, J. (1996) Separable Dual-Space Gaussian Pseudopotentials *Phys. Rev. B* 54**:** 1703.
33. Kuo, I. F. W., Mundy, C. J., McGrath, M. J., Siepmann, J. I., VandeVondele, J., Sprik, M., Hutter, J., Chen, B., Klein, M. L., Mohamed, F., Krack, M. & Parrinello, M. (2004) Liquid water from first principles: Investigation of different sampling approaches *J. Phys. Chem. B* 108**:** 12990-12998.
34. VandeVondele, J. & Hutter, J. (2003) An efficient orbital transformation method for electronic structure calculations *J Chem Phys* 118**:** 4365-4369.

35. Jungwirth, P., Curtis, J. E. & Tobias, D. J. (2003) Polarizability and aqueous solvation of the sulfate dianion *Chem. Phys. Lett.* 367**:** 704-710.
36. Caldwell, J. W. & Kollman, P. A. (1995) Structure and Properties of Neat Liquids Using Nonadditive Molecular-Dynamics - Water, Methanol, and N-Methylacetamide *Journal of Physical Chemistry* 99**:** 6208-6219.
37. Frisch, M. J., Trucks, G. W., Schlegel, H. B., Scuseria, G. E., Robb, M. A., Cheeseman, J. R., Zakrzewski, V. G., Montgomery, J. A., Jr., R. E. S., J. C. Burant & S. D.; J. M. Millam, A. D. D. K., K. N.; Strain, M. C.; Farkas, O.; Tomasi, J.; Barone, V.; Cossi, M.; Cammi, R.; Mennucci, B.; Pomelli, C.; Adamo, C.; Clifford, S.; Ochterski, J.; Petersson, G. A.; Ayala, P. Y.; Cui, Q.; Morokuma, K.; Malick, D. K.; Rabuck, A. D.; Raghavachari, K.; Foresman, J. B.; Cioslowski, J.; Ortiz, J. V.; Stefanov, B. B.; Liu, G.; Liashenko, A.; Piskorz, P.; Komaromi, I.; Gomperts, R.; Martin, R. L.; Fox, D. J.; Keith, T.; Al-Laham, M. A.; Peng, C. Y.; Nanayakkara, A.; Gonzalez, C.; Challacombe, M.; Gill, P. M. W.; Johnson, B.; Chen, W.; Wong, M. W.; Andres, J. L.; Gonzalez, C.; Head-Gordon, M.; Replogle, E. S.; Pople, J. A. *Gaussian 98, Rev A6; Gaussian Inc.:Pittsburgh PA, 1998.*
38. Wren, A. G., Phillips, R. W. & Tolentino, L. U. (1979) Surface-Reactions of Chlorine Molecules and Atoms with Water and Sulfuric-Acid at Low-Temperatures *J Colloid Interf Sci* 70**:** 544-557.
39. Copperthwaite, R. G. & Lloyd, J. (1977) Photoinduced Decomposition of Sodium-Perchlorate and Sodium-Chlorate When Studied by X-Ray Photoelectron-Spectroscopy *J Chem Soc Dalton***:** 1117-1121.
40. Stephen, H. & Stephen, T. (1963) (Pergamon Press, Oxford).

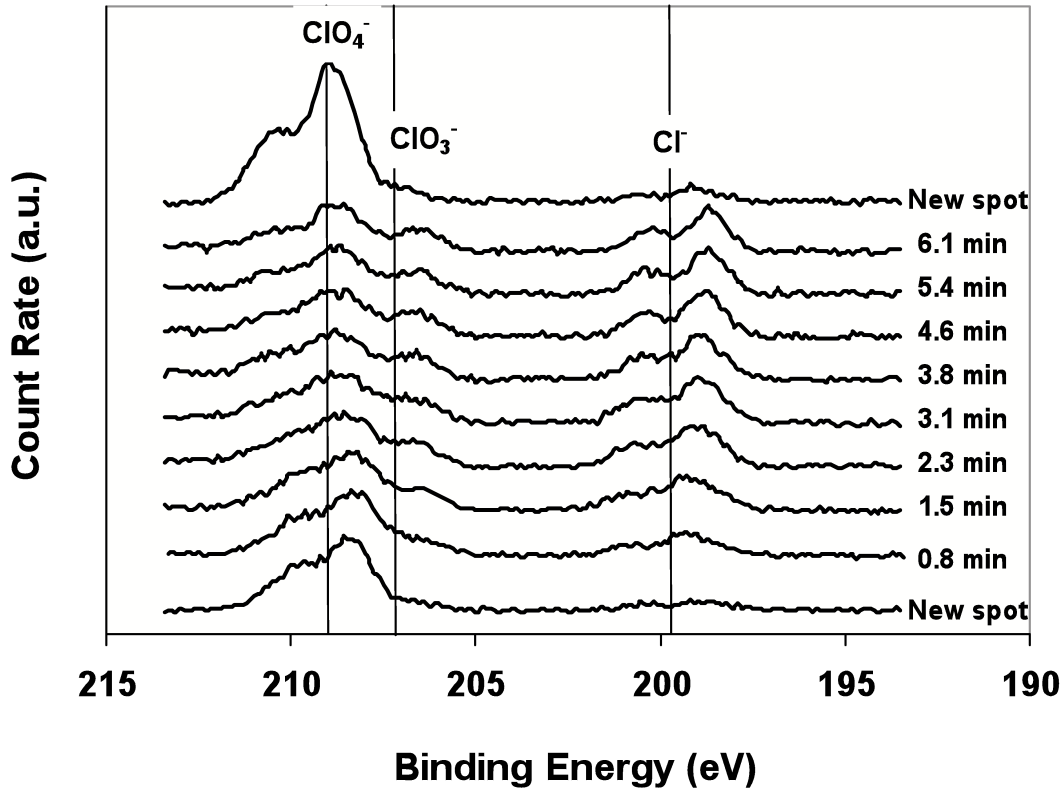

Fig 1. Ambient pressure XP spectra of the Cl(2p) region acquired sequentially at the same location on a $NaClO_4$ crystallite at a sample temperature of 21 °C and water vapor pressure of 1.6 Torr which corresponds to ~5% relative humidity condition. The incident photon energy is 500 eV which corresponds to a KE of 300 eV. The spectra have been charge referenced to the Na(2s) orbital set at 64.20 eV, characteristic of solid $NaClO_4$.

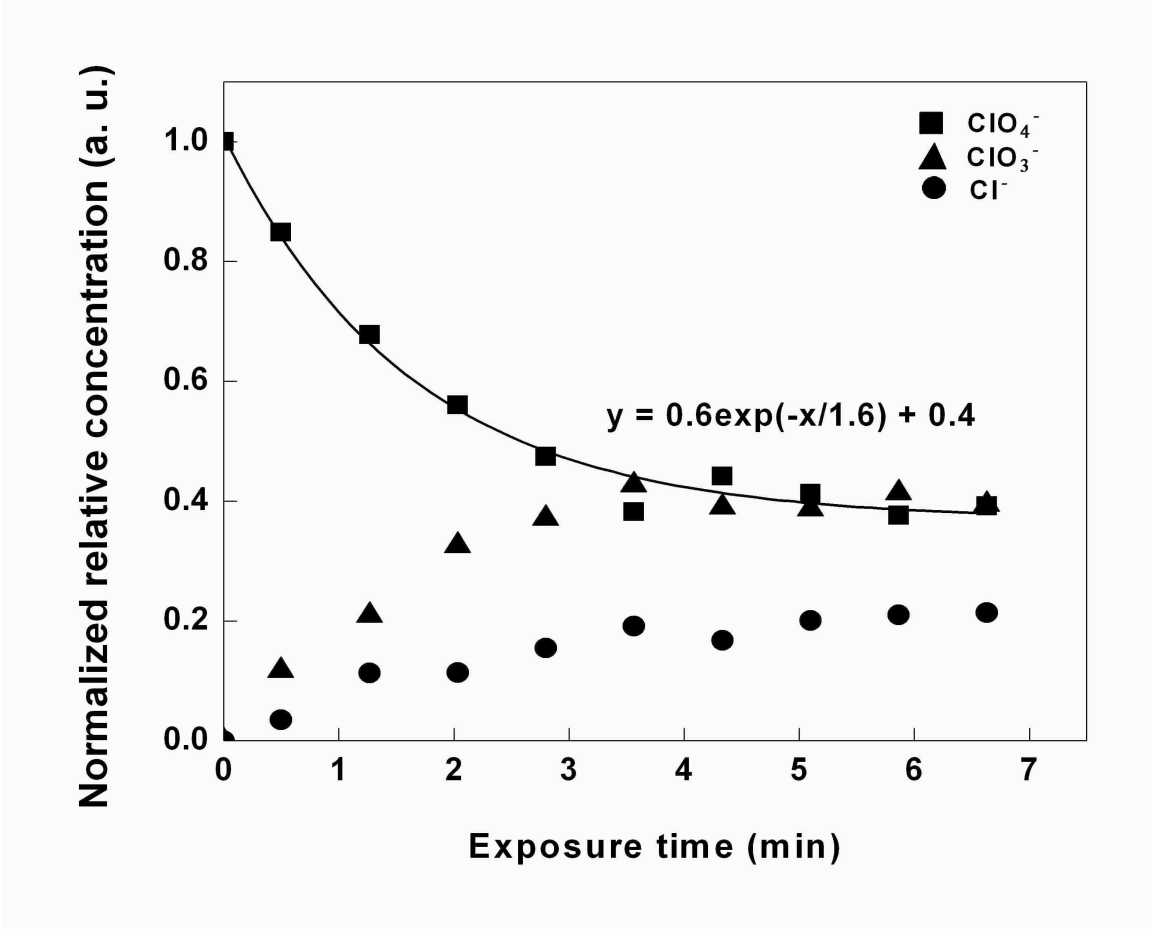

Fig. 2. Plot showing the normalized concentrations of ClO_4^-, ClO_3^-, and Cl^- species as a function of the x-ray exposure time. The trend line through ClO_4^- data points represents fit to a first order rate equation.

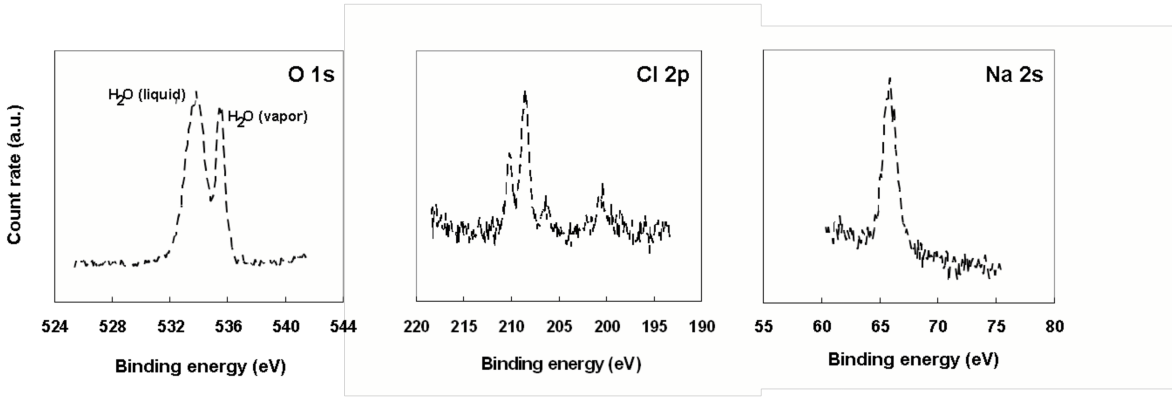

Fig. 3. AP-XP spectra of the O(1s), Cl(2p) and Na(2s) core levels for a saturated $NaClO_4$ solution at 200 eV photoelectron kinetic energy.

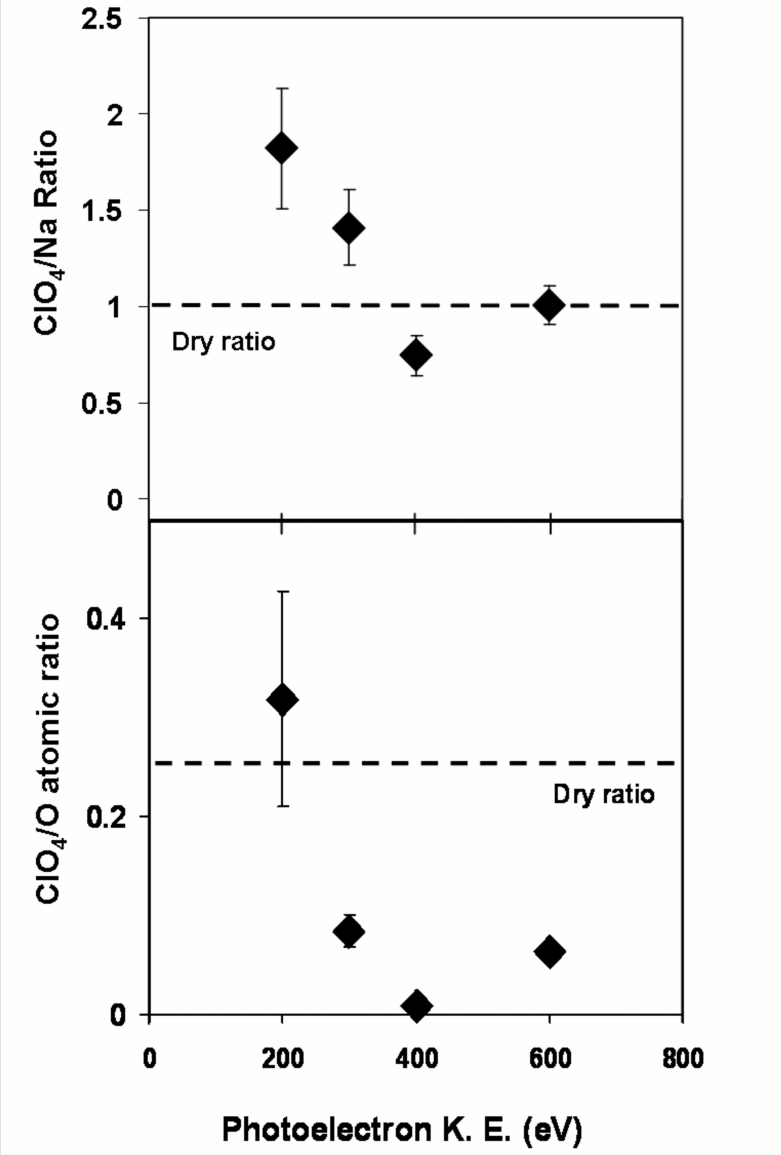

Fig 4. Plots showing the measured (A) ClO_4^-(Cl2p)/Na^+(Na2s) and (B) ClO_4^-(Cl2p)/O(O1s) ($H_2O_{(l)}$) ratio as a function of photoelectron kinetic energy for a saturated $NaClO_4$ aqueous solution. The average value of multiple measurements is shown, with the error bar representative of the standard error between sample spots. Each data point was collected on a fresh sample spot as a means to minimize the loss of halogen signal due to X-ray beam damage.

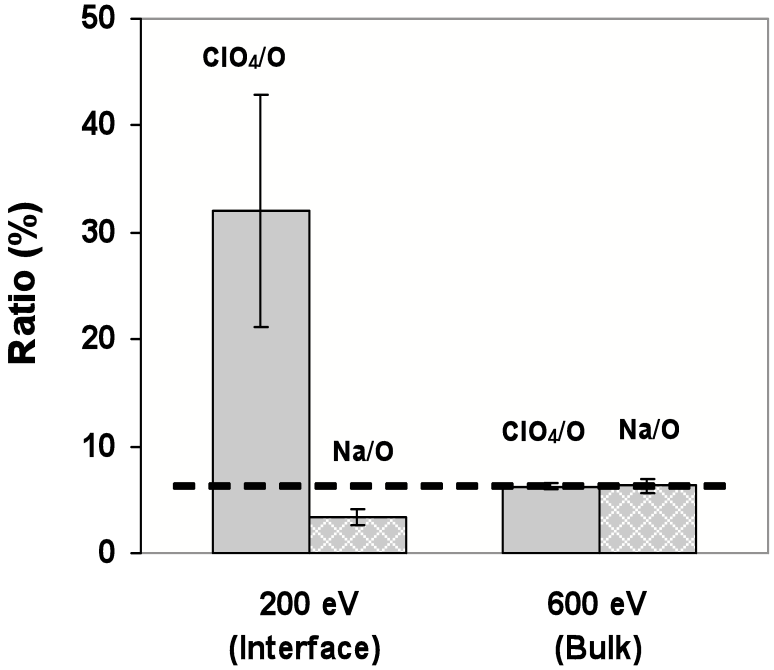

Fig. 5. Experimentally measured concentrations of ions in the saturated $NaClO_4$ solution for two different photoelectron kinetic energy: 200 eV (interface) and 600 eV (bulk). Error bars indicating standard error are shown for the experimental measurements. The dashed line indicates the expected concentrations of the ions based on thermodynamic data for bulk, saturated solutions.

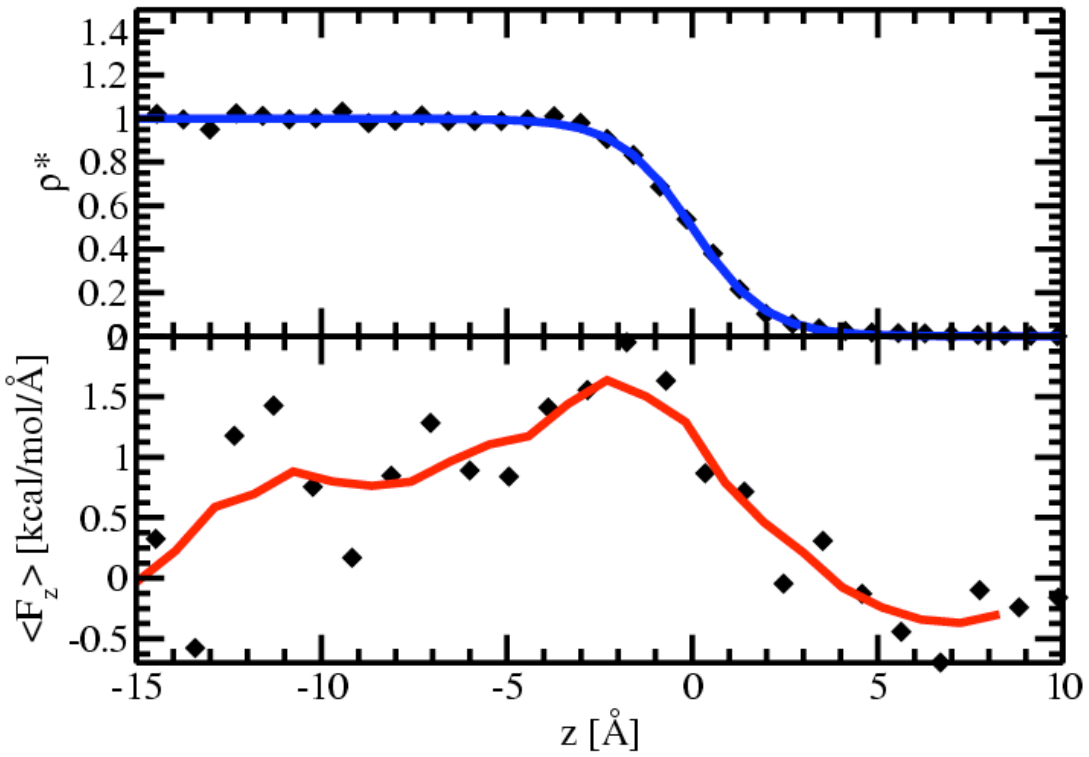

Fig. 6. Density profile in reduced units and average force obtained from first principles molecular dynamics simulations. The density profile was normalized to the fitted bulk density of the slab value of 0.845 g/ml. The Gibbs dividing surface was obtained from the density profile and set to 0.0 Å in the current figure. The red line represents the running average computed over 3 nearest data points.

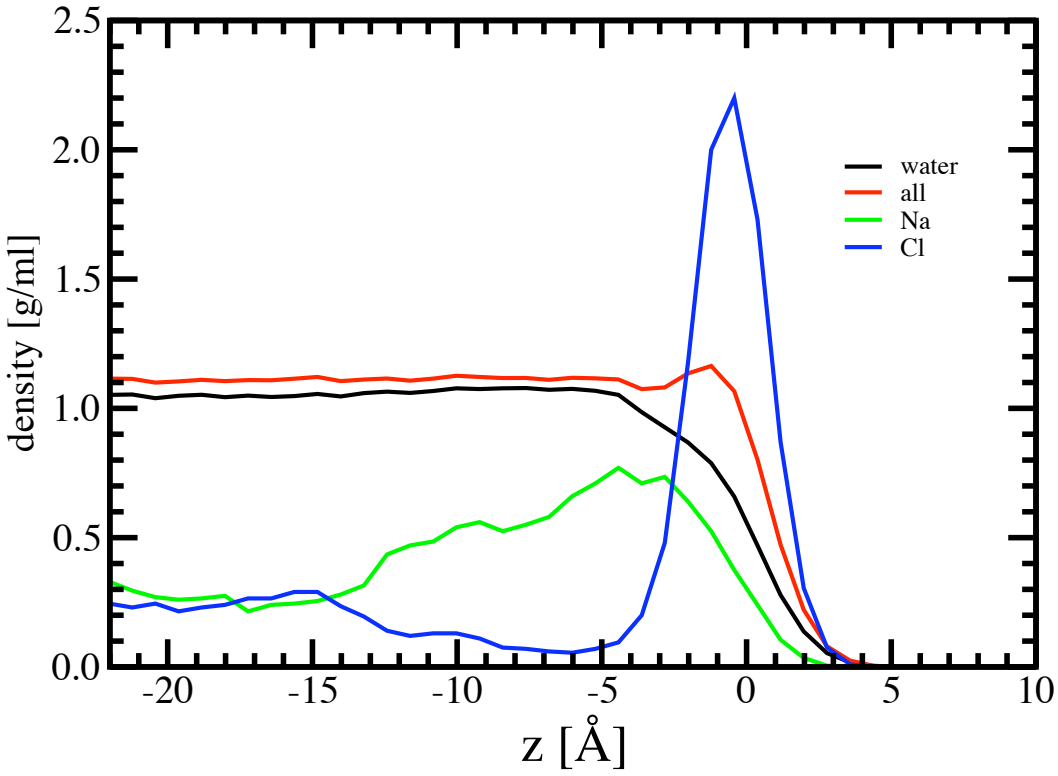

Fig. 7. Density profile obtained polarizable force field molecular dynamics simulation of a water slab containing 16 Na^+, 16 ClO_4^-, and 1054 water molecules. The Gibbs dividing surface is set to 0.0 Å

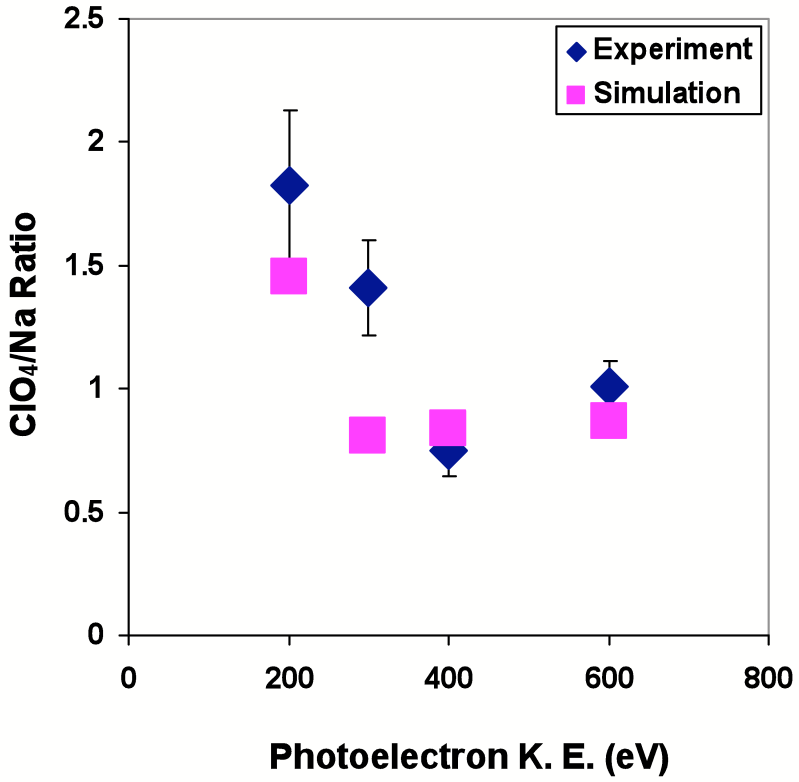

Fig. 8. The measured and predicted ClO_4^-/Na^+ atomic ratio as a function of photoelectron kinetic energy. The blue diamonds are the experimental results corresponding to the saturated $NaClO_4$ solution, while the magenta squares are the atomic ratio calculated from the MD simulation. The predicted atomic ratio is calculated by integration of a convolution integral for each ion.

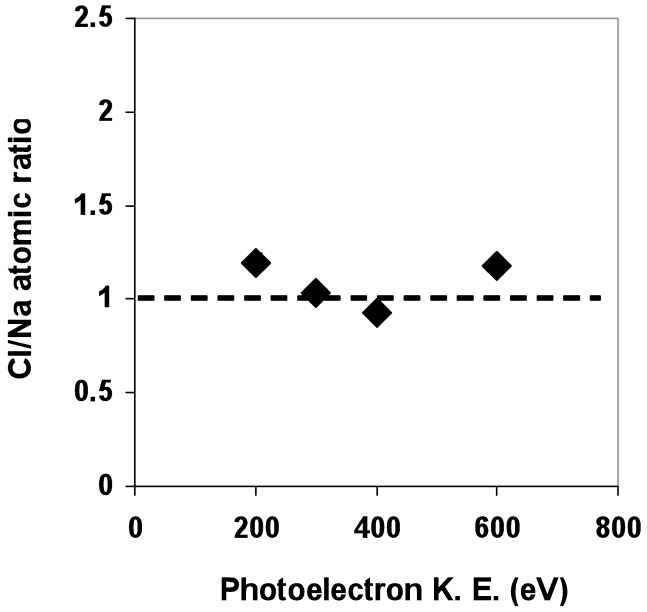

Fig. 9. Plots showing the measured (A) Cl^{-}(Cl2p)/Na^{+}(Na2s) ratio as a function of photoelectron kinetic for a saturated NaCl aqueous solution. The average value of multiple measurements is shown, with the error bar representative of the standard error between sample spots. Each data point was collected on a fresh sample spot as a means to minimize the loss of halogen signal due to X-ray beam damage.